Regulation of Anti–double-stranded DNA B Cells in Nonautoimmune Mice: Localization to the T–B Interface of the Splenic Follicle

By Laura Mandik-Nayak, Anh Bui, Hooman Noorchashm, Ashlyn Eaton, and Jan Erikson

From The Wistar Institute, Philadelphia, Pennsylvania 19104

Summary

Systemic lupus erythematosus (SLE) and the MRL-*lpr*/*lpr* murine model for SLE are characterized by the presence of serum anti–double-stranded (ds)DNA antibodies (Abs), whereas nonautoimmune individuals have negligible levels of these Abs. To increase the frequency of anti-DNA B cells and identify the mechanisms involved in their regulation in nonautoimmune mice, we have used Ig transgenes (tgs). In the present study, we used the VH3H9 heavy (H) chain tg which expresses an H chain that was repeatedly isolated from anti-dsDNA Abs from MRL-*lpr*/*lpr* mice. Because the VH3H9 H chain can pair with endogenous L chains to generate anti–single-stranded DNA, anti-dsDNA, and non-DNA B cells, this allowed us to study the regulation of anti-dsDNA B cells in the context of a diverse B cell repertoire. We have identified anti-dsDNA B cells that are located at the T–B interface in the splenic follicle where they have an increased in vivo turnover rate. These anti-dsDNA B cells exhibit a unique surface phenotype suggesting developmental arrest due to antigen exposure.

Ig transgenic models to neo-self Ags have helped to classify two manifestations of B cell tolerance: clonal deletion and functional inactivation (anergy) (1–3). Recently, the distinction between these two has come into question as "anergized" cells have been shown to have a reduced lifespan and may be in a state of "delayed deletion" (4). Furthermore, the relative contribution of deletion versus receptor editing to the elimination of autoreactive B cells is being reevaluated (5, 6). Given that most autoimmune diseases are characterized by the presence of autoantibodies directed toward a discrete set of autoantigens, we are interested in determining whether the mechanisms described for the maintenance of tolerance to neo-self Ags apply to disease-associated autoantigens.

Anti–double-stranded (ds)[1] DNA Abs are one of the hallmarks of SLE and the MRL-*lpr*/*lpr* murine model for SLE, and rising titers of these Abs correlate with disease exacerbation (7). In the serum of nonautoimmune individuals, anti-dsDNA Abs are not present, suggesting that this specificity is regulated, yet the mechanism governing this regulation remains unclear. To follow the fate of anti-dsDNA B cells, we have used Ig transgenic mice. The transgene (tg) being studied encodes the VH3H9 H chain, originally isolated from anti-dsDNA Igs in diseased MRL-*lpr*/*lpr* mice, in combination with different L chains (8). Transfection studies have shown that this H chain can pair with a variety of different L chains to generate both anti–single-stranded (ss)DNA and anti-dsDNA Abs (9). As a tg, VH3H9 can pair with endogenous L chains to generate anti-ssDNA, anti-dsDNA, and non-DNA B cells, allowing us to study the regulation of anti-dsDNA B cells in the presence of B cells with other specificities (10, 11). Tracking anti-dsDNA B cells in a diverse repertoire is important because this more closely mimics the conditions present in SLE. In addition, precedent exists for a differential fate of autoreactive B cells in the context of a monoclonal versus polyclonal B cell repertoire (12, 13).

There have been conflicting reports on the fate of anti-dsDNA B cells in nonautoimmune mice. Some state that anti-dsDNA B cells are deleted in the bone marrow; others report that these cells exit to the periphery, but do not secrete anti-dsDNA Ab due to endogenous Ig expression or B cell functional inactivation (14–17). These discrepancies may be a reflection of the degree to which individual Ig tgs are capable of inhibiting endogenous Ig rearrangement, which could rescue an otherwise autoreactive B cell. Whether endogenous Ig expression is due to the active induction of receptor editing or is the consequence of a defect on the part of the Ig tgs to inhibit rearrangement can be difficult to assess, particularly for L chain tgs (15–19). A

[1] *Abbreviations used in this paper:* AP, alkaline phosphatase; BrdU, bromodeoxyuridine; ds, double-stranded; HEL, hen egg lysozyme; HRP, horseradish peroxidase; HSA, heat-stable antigen; MFI, mean fluorescence intensity; PALS, periarteriolar lymphoid sheath; ss, single-stranded; tg, transgene; V, variable.

 J. Exp. Med. © The Rockefeller University Press • 0022-1007/97/10/1257/11 $2.00
Volume 186, Number 8, October 20, 1997 1257–1267
http://www.jem.org

more interesting possibility to explain these divergent outcomes is that they reflect the different specificities of the tgs used in these studies, which may in turn differ in their regulation (14–17, 20). Because anti-dsDNA Abs from SLE patients and lupus mice are heterogeneous, and the particular specificities which are significant in disease are not known, it will be important to understand these differences (21, 22).

The VH3H9 tg offers an opportunity to study the regulation of a range of anti-DNA B cells. Initial studies using the VH3H9 H chain tg on the BALB/c background demonstrated that neither anti-ssDNA nor anti-dsDNA serum Abs were elevated over tg(−) BALB/c control sera (23). When hybridoma panels were generated from the spleens of VH3H9 tg mice, anti-ssDNA and non-DNA hybridomas were recovered, but not anti-dsDNA hybridomas (23, 24). Transfection studies clearly showed that this H chain has the capacity to generate anti-dsDNA B cells (9). Importantly, we have also recovered this specificity in hybridoma panels generated from VH3H9 MRL-*lpr*/*lpr* spleens (10). The absence of anti-dsDNA hybridomas from BALB/c-derived panels suggests, therefore, that they are either deleted in the bone marrow or, if present, cannot be rescued as hybridomas.

To address the mechanisms governing the regulation of anti-dsDNA B cells in a diverse repertoire and to avoid the use of L chain tgs altogether, we relied on the fact that VH3H9 can pair with endogenous Vλ1 L chains to generate anti-dsDNA Abs (9). Thus, we were able to track the λ1-bearing anti-dsDNA B cells in the context of the diverse repertoire of the VH3H9 tg mouse. We have found that anti-dsDNA B cells are not deleted in the bone marrow, but instead exit to populate the spleen. Their unique surface phenotype suggests that they are both developmentally arrested and antigen experienced. These cells exhibit an increased in vivo turnover rate and are localized to the T–B interface of the splenic white pulp.

Materials and Methods

Mice

BALB/c mice were purchased from Harlan Sprague Dawley (Indianapolis, IN). VH3H9 tg mice have been described previously (23). The VH3H9 tg mice have been backcrossed onto the BALB/c background for at least nine generations, and have been bred and maintained in the animal facility at The Wistar Institute (Philadelphia, PA). In all cases, age-matched BALB/c mice or tg(−) littermates were used as controls. The presence of the VH3H9 tg was determined by PCR amplification of tail DNA with primers specific for VH3H9 (23).

Cell Preparations

Bone marrow, spleen, and lymph node cells were removed from VH3H9 tg and tg(−) mice. Single-cell suspensions were prepared and, where necessary, erythrocytes were removed by hypotonic lysis.

Flow Cytometry Analysis

Cells (5×10^5) were surface stained according to standard protocols (25). The following Abs were used: RA3-6B2-PE or biotin (anti-B220), R11-153-FITC (anti-Vλ1), R26-46-FITC or -biotin (anti-Vλ total), R8-140-PE (anti-Igκ), 1D3-FITC (anti-CD19), 7G6-FITC (anti-CD21), Cy34.1-FITC (anti-CD22), 3/23-FITC (anti-CD40), Mel-14-FITC (anti-CD62L, l-selectin), 2G9-PE (anti–I-A^d/I-E^d, MHC class II), M1/69-FITC (anti–heat-stable antigen [HSA]), IM7-FITC (anti-CD44) (all from PharMingen, San Diego, CA), LS136-biotin (anti-Vλ1), and JC5.1-PE (anti-Vλ total) (LS136 and JC5.1, gifts from J. Kearney, University of Alabama, Birmingham, AL; JC5-PE, gift from R. Hardy, Fox Chase Cancer Center, Philadelphia, PA), polyclonal anti-IgM-PE and SBA-1-PE (anti-IgD) (Southern Biotechnologies, Birmingham, AL), B3B4-FITC (anti-CD23) (gift from D. Conrad, Virginia Commonwealth University, Richmond, Virginia), and streptavidin-Red670 (GIBCO BRL, Gaithersburg, MD).

All samples were analyzed on a FACScan® flow cytometer (Becton Dickinson, Mountain View, CA) using Cellquest software. 15,000–40,000 events were collected for each sample and gated for live lymphocytes based on forward and side scatter.

Bromodeoxyuridine Labeling

8-d Labeling. Mice were injected intraperitoneally with 200 μl of 3 mg/ml 5-bromodeoxyuridine (BrdU) (Sigma Chemical Co., St. Louis, MO) in PBS every 12 h for 8 d. BrdU staining was performed essentially as described (26), with the exception that the cells were not fixed in ethanol. In brief, spleen and bone marrow cells from mice were isolated and surface stained as described above. The cells were then fixed and permeabilized with 1% paraformaldehyde containing 0.1% Tween-20. The DNA was denatured using 10 μM HCl and 100 U/ml DNase I. The incorporated BrdU was then detected using an anti-BrdU-FITC Ab (B44) from Becton Dickinson.

2-h Pulse. Mice were injected intraperitoneally with 200 μl of 3 mg/ml BrdU in PBS. The spleen and bone marrow cells were isolated 2 h later and stained as above.

Immunohistochemistry

Spleens were suspended in OCT, frozen in 2-methyl-butane cooled with liquid nitrogen, sectioned, and fixed with acetone. The spleen sections were stored at −70°C and then stained according to the protocol described (27). In brief, the sections were blocked using PBS/5% BSA/0.1% Tween 20, and then stained with GK1.5-biotin (anti-CD4), 53-6.7-biotin (anti-CD8), RA3-6B2-biotin (anti-B220) (grown as supernatants), and/or anti-Igλ-alkaline-phosphatase (AP; Southern Biotechnologies). Streptavidin–horseradish-peroxidase (HRP; Southern Biotechnologies) was used as a secondary antibody with the biotinylated reagents. HRP and AP were developed using the substrates 3-amino-9-ethylcarbazole and Fast-Blue BB base (Sigma Chemical Co., St. Louis, MO), respectively.

Hybridoma Generation

Spleen cells from a VH3H9 tg mouse were stained for B220, IgM, and CD44, and sorted for IgM^{low} $CD44^{high}$ cells (which includes VH3H9/Vλ1 anti-dsDNA B cells) by flow cytometry. The IgM^{low} $CD44^{high}$ cells were then cultured overnight in media (DMEM/10% FCS) containing CD40 ligand–CD8 fusion protein (a gift of P. Lane, Basel Institute for Immunology, Basel, Switzerland; reference 28; 1:2 dilution of culture supernatant) and rIL-4 (2 ng/ml; Genzyme Diagnostics, Cambridge, MA). The cells were then fused to the Ig(−) myeloma Sp2/0. Cells were plated at limiting dilution and wells bearing single colonies were expanded for analysis.

ELISA Assay. The Ig isotype of hybridomas was determined via an indirect solid-phase ELISA assay, using anti-IgH + L (Southern Biotechnologies) as the primary Ab and developing with AP-labeled anti-IgM, -IgG, -Igκ, or -Igλ Abs (Southern Biotechnologies). Binding to dsDNA was detected in a similar manner. In this case, the plates were coated with Avidin-DX (Vector, Burlingame, CA); DNA-biotin was used in place of the primary antibodies. DNA-biotin was prepared as described (9).

Sequence Analysis. The H and L chain variable (V) regions were sequenced from messenger RNA according to the protocol described (29). In brief, cytoplasmic RNA was isolated and constant region–specific primers were used to direct synthesis of cDNA copies of the H (Cμ1) and L (Cλ1) chain V regions. The cDNA was then amplified using the constant region primers in conjunction with VH5′1 or λ1L primers that hybridize to the 5′ ends of H and L chain V region genes, respectively (29). Amplification products were sequenced by automated analysis (Wistar Institute Nucleic Acid Facility). Sequence translation and comparison was carried out using the Sequencher program and by searching EMBL/GenBank/DDBJ databases.

Antinuclear Antibody Assay. The presence of antinuclear antibodies in the supernatants was detected using permeabilized HEP-2 cells as the substrate (Antibodies Incorporated, Davis, CA). The supernatants were used undiluted and were detected using an anti–mouse IgM or IgH + L–FITC secondary Ab (Southern Biotechnologies). The samples were then visualized under a fluorescent microscope.

Statistical Analysis. Statistical significance was determined using an unpaired Student's *t* test and Instat Software.

Results and Discussion

Anti-dsDNA B Cells Are Present in the Periphery of Nonautoimmune Mice. In this study, we use VH3H9 H chain only tg mice to increase the frequency of anti-dsDNA B cells while maintaining a polyclonal repertoire. Transfection and hybridoma analysis have identified germline Vλ1 as an L chain that pairs with the VH3H9 H chain to generate an anti-dsDNA Ab (see J558LT and MRL1-45 in Table 1; references 9, 10). Because the VH3H9 H chain tg has been shown to be a good excluder of endogenous H chain rearrangement on the BALB/c background (Table 1; references 23, 30), we can follow the fate of anti-dsDNA B cells in VH3H9 tg mice using anti-λ specific reagents. Several different reagents were used to track λ^+ and $\lambda1^+$ B cells (LS136, R11-153, JC5, and R26-46). Using these reagents and flow cytometry, we have shown that the majority of λ^+ B cells in VH3H9 tg mice are λ1 (79 ± 19%). Therefore, for the remainder of our studies, we have used anti-pan λ reagents to detect anti-dsDNA B cells. As is shown in Fig. 1, λ^+ B cells are present in the bone marrow, spleen, and lymph node. It is also apparent that the levels of λ Ig on these cells are lower in the periphery compared to λ^+ B cells from tg(−) mice (spleen: mean fluorescence intensity [MFI] 52 versus 181; LN: MFI 52 versus 216). Interestingly, Ig levels are also decreased on the λ^+ B cells from the bone marrow (MFI 47 versus 197). There is precedent for antigen encounter leading to a decrease in Ig density in other tolerance model systems; for example, anti–hen egg lysozyme (HEL) B cells have a reduced level of Ig when in the presence of HEL (3), but when these B cells are removed from Ag, either by in vivo parking or in vitro cultures, their surface Ig levels increase (31, 32). The decreased Ig density on the anti-dsDNA B cells suggests that these cells are encountering their Ag and that this encounter initially occurred in the bone marrow.

One scenario that could account for the presence of λ^+ B cells in the periphery of VH3H9 tg mice is coexpression of a kappa chain or an endogenous H chain to generate a non-dsDNA–binding Ab (10, 15, 33, 34). Indeed, our previous analysis of hybridomas generated from either unmanipulated or LPS-activated B cells from VH3H9 BALB/c mice detected a single λ^+ hybrid (BALB1-72) that also coexpressed a kappa protein (Table 1). The addition of the second L chain (kappa) disrupted DNA binding, which we suggested most likely spared the B cell from deletion (10). A similar scenario has been described for VH3H9 tg mice bred to Vκ4 tg mice (15). VH3H9/Vκ4 encodes an anti-dsDNA Ig, but no peripheral B cells with this specificity were identified in the tg mice. The fact that all the B cells isolated as hybridomas coexpressed an endogenous L chain was interpreted as evidence for receptor editing (15). In contrast, the λ^+ B cells we detect show no evidence of L chain coexpression by flow cytometry; the B cells all express either κ or λ (data not shown). Because low levels of surface Ig are hard to detect using flow cytometry, we took a second approach; B cells were isolated by flow cytometry based on Ig density, cultured in a cocktail mimicking T help (CD40 ligand and rIL-4), and then used to generate hybridoma panels. Anti-dsDNA hybridomas were recovered that only expressed a λ L chain as detected by ELISA.

Table 1. *λ-expressing Hybridomas: Specificity and Ig Usage*

	L chains			H chains		Specificity	
Hybridoma	κ*	λ*	λ1‡	VH3H9‡	endog.Ig‡	dsDNA§	ANA
J558LT‖	−	+	+	+	−	+	+
MRL1-45¶	−	+	+	+	−	+	+
BALB1-72¶	+	+	+	+	−	−	−
L1	−	+	+	+	−	+	+
L9	−	+	+	+	−	+	+
L12	−	+	+	+	−	+	+
L17	−	+	+	+	−	+	+

ANA, antinuclear antibody; endog, endogenous.

*The presence of κ and λ protein was determined by ELISA performed on hybridoma supernatants. An OD of 5× background was considered positive.

‡L and H chain genes were sequenced as described in Materials and Methods.

§Binding to dsDNA was assessed by ELISA on hybridoma supernatants. An OD of 4× background was considered positive.

‖J558LT is the previously published VH3H9/λ1 transfectant and is shown here as a positive control (9).

¶MRL1-45 and BALB1-72 were described previously and are shown here for comparison (10).

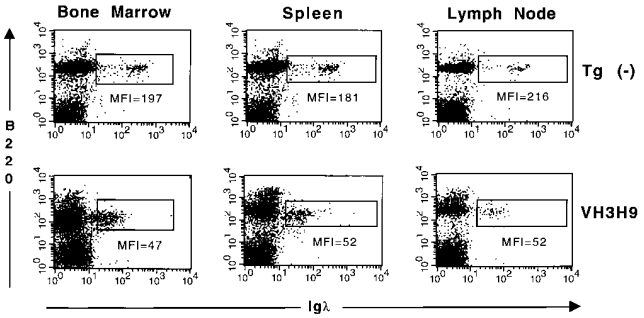

Figure 1. VH3H9/λ anti-dsDNA B cells are present with a reduced Ig density. Bone marrow (*left*), spleen (*middle*), and lymph node (*right*) cells from Tg(−) (*top*) and VH3H9 tg (*bottom*) mice were stained with anti-B220-biotin/streptavidin-Red670 and anti-λ-FITC. MFI is given for the λ^+ cells in the boxed region. These are representative plots of $n = 19$ mice of each genotype.

Importantly, messenger RNA H + L sequencing analysis showed that these hybridomas exclusively use the VH3H9 tg and Vλ1 (Table 1). The ability to rescue anti-dsDNA B cells with T help–derived factors is intriguing in light of the requirement for T cells in murine SLE (35–37). In addition, this may explain why we, and others, did not previously recover anti-dsDNA B cells from LPS-derived hybridomas (10, 14, 23, 24, 34).

Anti-dsDNA B Cells Are Developmentally Arrested and Show Signs of Antigen Experience. Using flow cytometry, we as-

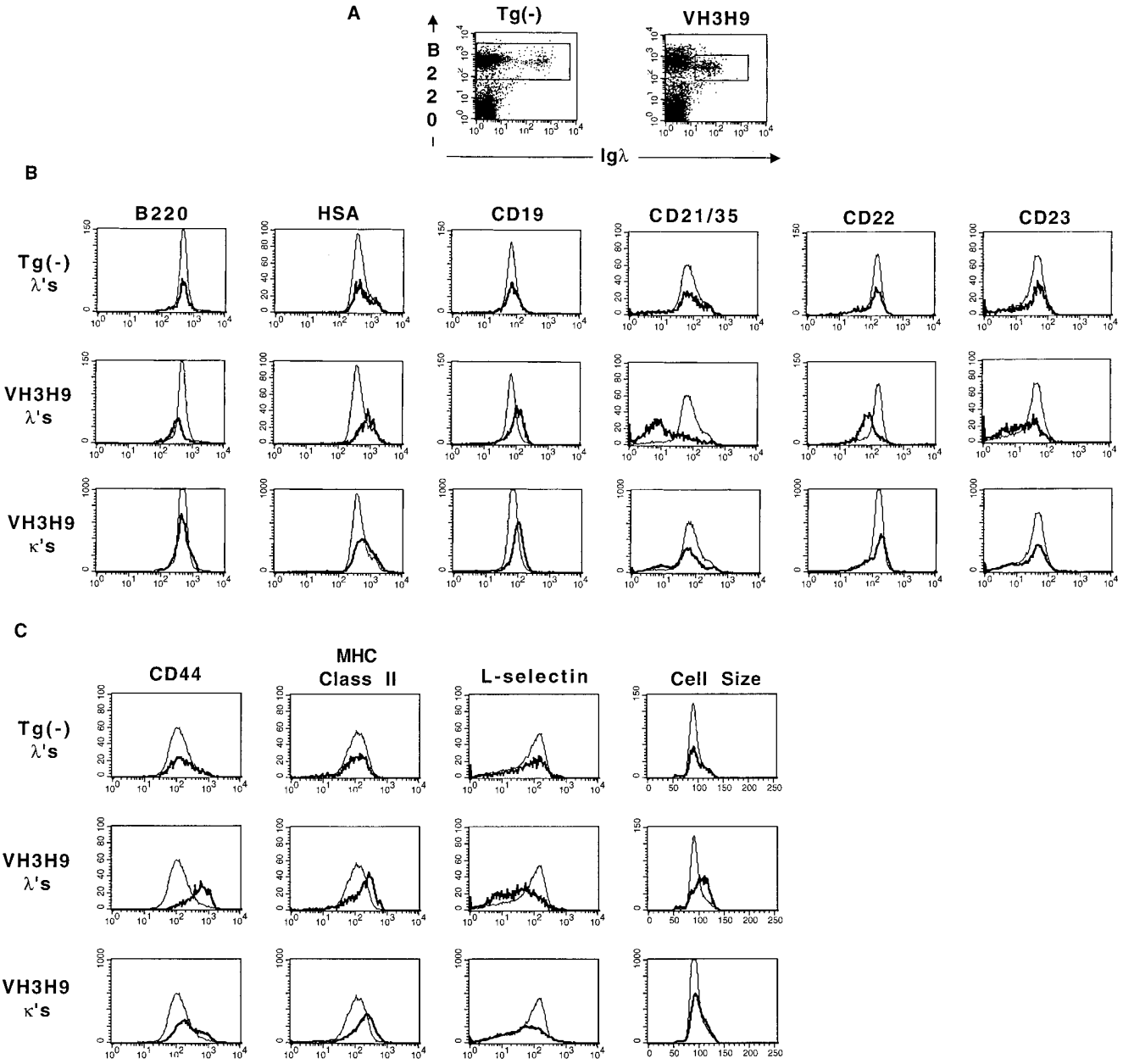

sessed the developmental and activation status of anti-dsDNA B cells in the spleen. The panel of developmental markers, shown in Fig. 2, includes CD19, CD21/35, CD22, CD23, HSA, and B220. We compared the expression levels of these markers on λ^+ B cells from VH3H9 tg mice with those on the tg(−) λ^+ B cells, as well as the total B cell population, from tg(−) mice (Fig. 2). B220 (CD45R) increases with maturity and, in conjunction with HSA, has been used to define the immature to mature stages of B cell development (25). HSA is expressed at high levels on immature (newly emerging) B cells and at a lower level on mature B cells in the spleen (26). As is shown in Fig. 2 *B*, the VH3H9/λ B cells express a slightly reduced level of B220 and a level of HSA intermediate between the HSA^{high} and HSA^{low} cells in the tg(−) spleen. CD22 is expressed at a low level on immature B cells and increases with maturity, whereas CD21/35 and CD23 become surface positive at the mature B cell stage (38–41). The VH3H9/λ B cells have a dramatically reduced level of CD21/35, as well as lower levels of CD22 and CD23 on their surface (Fig. 2 *B*). Because CD21/35 (complement receptors 1 and 2) and CD22 play a role in modulating the response through the Ig receptor (42–45), the low expression levels of these coreceptors on VH3H9/λ B cells may alter the signaling threshold of these cells when stimulated through membrane Ig. CD19 is a B cell–specific marker that is expressed on all B cells starting at the pro–B cell stage (46). As is shown in Fig. 2 *B*, CD19 expression on the surface of λ^+ B cells in VH3H9 tg mice is higher than on B cells from tg(−) mice. CD40 was also examined and has a similar expression level to tg(−) B cells (data not shown). In contrast to VH3H9 tg mice, the λ^+ B cells in tg(−) mice have equivalent levels of all surface markers tested (Fig. 2), suggesting that there is nothing inherently different about B cells with λ L chains. Taken together, these data suggest that the VH3H9/λ B cells are phenotypically immature.

As an indication of activation/antigen encounter, additional cell surface markers, whose differential expression levels have been used to mark a B cell's activation state, were also analyzed. CD44 and MHC class II are molecules whose expression levels increase on activated B cells (47–49). l-selectin expression decreases upon activation, but given that it is also low on immature B cells, it cannot be used to distinguish an immature B cell from a postactivated one (50, 51). The λ^+ B cells in VH3H9 tg mice express increased levels of CD44 and MHC class II and decreased

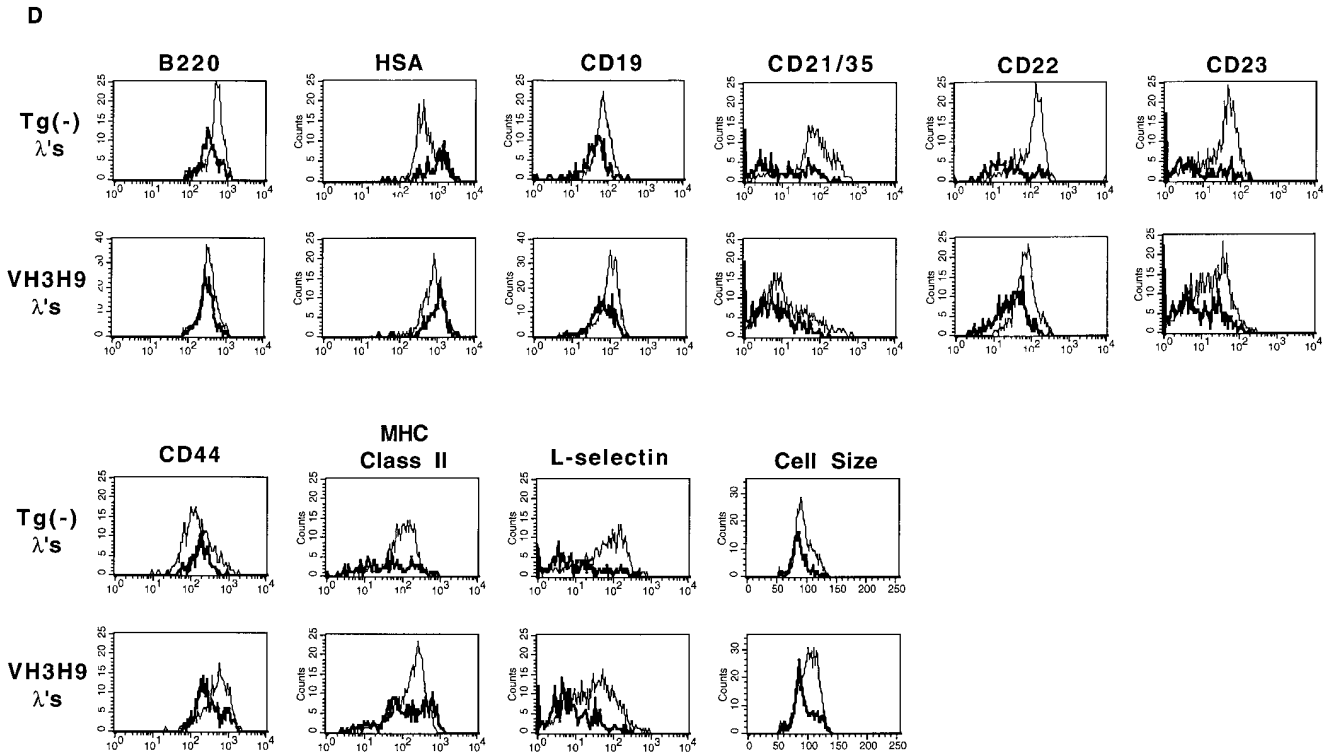

Figure 2. Phenotypic analysis of VH3H9/λ B cells. Spleen (*A–C*) and bone marrow (*D*) B cells were stained with anti-B220-biotin/streptavidin-Red670, anti-λ-PE or -FITC, and either anti-HSA, CD19, CD21/35, CD22, CD23, CD44, CD62L-FITC, or anti–class II–PE. (*A*) Dot plots showing B220 versus λ staining in the spleen. (*B*) Developmental markers and (*C*) activation markers on the total splenic B cell population (gating on $B220^+$ cells) in tg(−) mice (*thin lines* in *B* and *C*) and $B220^+\lambda^+$ B cells in tg(−) mice (*bold line*, *top*), $B220^+\lambda^+$ B cells in VH3H9 mice (*bold line*, *middle*), or $B220^+\kappa^+$ B cells in VH3H9 tg mice (*bold line*, *bottom*). The underlayed histograms (*thin lines*) were scaled down to allow for the comparison to the λ+ B cells (which are present at ~0.1 the frequency of total B cells) in the upper and middle panels. (*D*) Histograms showing developmental and activation markers on the λ+ B cells in the spleen (*thin line*) and bone marrow (*bold line*) in tg(−) (*top panels*) and VH3H9 tg mice (*bottom panels*). These are representative plots from $n = 4$ mice of each genotype.

levels of l-selectin (Fig. 2 *C*). Together, these data as well as the increase in cell size (Fig. 2 *C*), suggest that the anti-dsDNA B cells have encountered antigen.

To determine at what point anti-dsDNA B cells have been arrested in development, flow cytometric analysis of VH3H9/λ^+ bone marrow cells was performed. The majority of λ^+ B cells in the bone marrow of VH3H9 tg mice express similar levels of the markers B220, HSA, CD21, CD22, CD23, CD44, and l-selectin as the tg(−) bone marrow B cells (compare the bold lines in Fig. 2 *D*). Additionally, in comparison to the bone marrow, the VH3H9/λ B cells in the spleen have altered their expression level of B220, HSA, CD22, CD23, and l-selectin, consistent with their continued maturation (compare the thin line to the bold line in Fig. 2 *D*). These data suggest that B cell development proceeds in the bone marrow for the VH3H9/λ^+ cells in a similar fashion to λ^+ cells from tg(−) mice, and furthermore, that the λ^+ anti-dsDNA B cells in the spleen have matured more than the majority of bone marrow B cells.

VH3H9 tg mice contain, in addition to anti-DNA B cells, a population of non-DNA B cells in the repertoire that allow us to control for and distinguish effects which are due to autoreactive specificity versus those that are due to the presence of the transgene (10, 23). The presence of non-DNA B cells in VH3H9 tg mice would predict that not all of the B cells in these mice will exhibit the immature/activated phenotype. Indeed, comparing the surface phenotype of the κ^+ cells in the VH3H9 tg mice with B cells from tg(−) mice shows that the majority of the VH3H9 κ^+ B cells express cell surface densities equivalent to their tg(−) counterparts for both the developmental markers (CD21/35, CD22, CD23, B220, and HSA; Fig. 2 *B*) as well as activation markers (CD44, l-selectin, and cell size; Fig. 2 *C*). In contrast, CD19 and MHC class II are slightly elevated on all of the VH3H9 cells (Fig. 2, *B* and *C*), implying that their alteration may be due to the presence of VH3H9 tg per se, and not to their autoreactive specificity. Furthermore, as transfection studies and L chain repertoire analysis of hybridoma panels from VH3H9 tg MRL-*lpr*/*lpr* mice have revealed, there are κ L chains in addition to λ1, which can pair with the VH3H9 H chain to generate anti-dsDNA B cells (8–10). We predicted that these B cells would also be regulated and exhibit an altered surface phenotype. Consistent with this, there is a small population of VH3H9 κ^+ B cells that exhibit a phenotype similar to the VH3H9/λ^+ B cells: CD21/35^{low}, CD22^{low}, CD23^{low}, CD44^{high}, and l-selectin^{low} (note the shoulders in Fig. 2, *B* and *C*).

In summary, the VH3H9/λ1 anti-dsDNA B cells have a unique cell surface phenotype, as does a subpopulation of VH3H9/κ B cells. They show evidence of activation (CD44^{high}, l-selectin^{low}, and increased cell size), suggesting that they have been exposed to Ag. In addition, they appear developmentally arrested in that they express reduced levels of CD21/35, CD22, CD23, l-selectin, and B220, and intermediate levels of HSA. These data suggest that anti-dsDNA B cells have encountered their Ag while still at an immature stage, resulting in arrested development with respect to some markers and a concurrent change in the expression of activation markers. In support of this, there is a reduced level of surface Ig in the bone marrow (Fig. 1). A similar immature phenotype (low levels of CD21/35, CD22, CD23, and l-selectin) was seen in the anti-HEL/membraneHEL mice in the context of a bcl-2 tg, whereas in the absence of the bcl-2 tg, the anti-HEL B cells were deleted

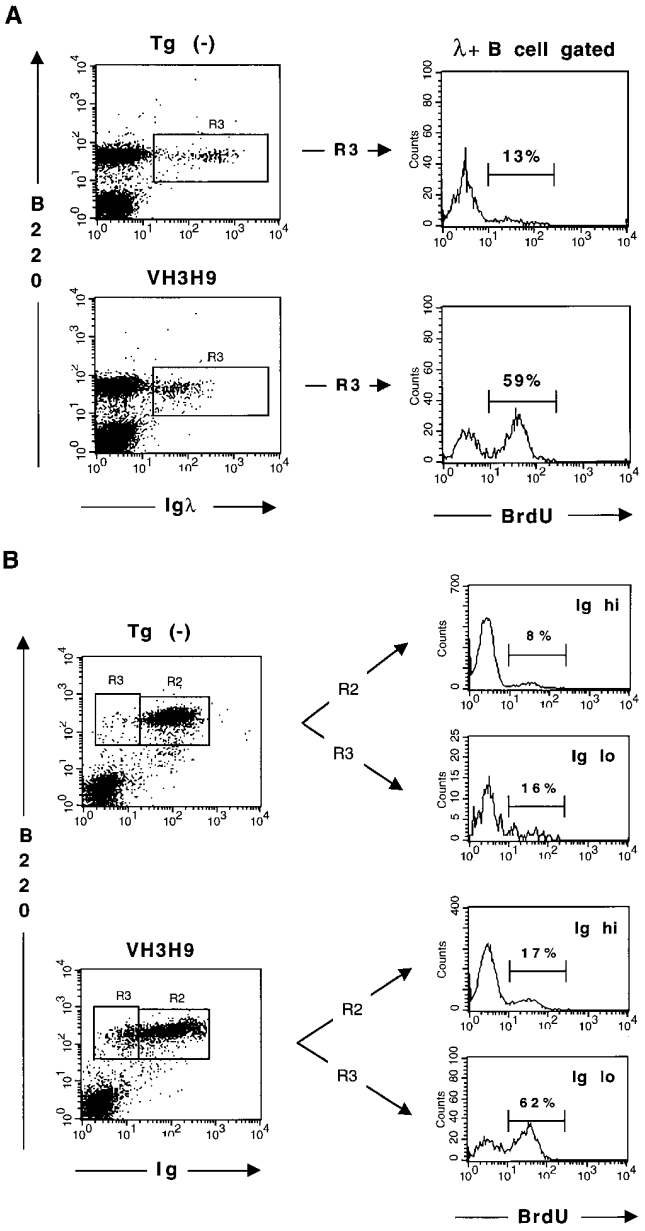

Figure 3. VH3H9/λ B cells have an increased in vivo turnover rate. Tg(−) (*top*) and VH3H9 (*bottom*) mice were continuously labeled with BrdU for 8 d. Spleen cells were then stained with anti-λ-biotin/streptavidin-Red670 and anti-B220-PE or anti–IgM + IgD–PE (*Ig*), fixed, permeabilized, and then incorporated BrdU was detected with anti-BrdU Ab. (*A*) Dot plots show B220 versus λ (*left*) and histograms show BrdU label within the B220$^+\lambda^+$ gate (*right*). Percentages are given for the BrdU$^+$ cells. (*B*) Dot plots show B220 versus Ig (*left*) and histograms show BrdU label for the indicated B220$^+$Ig^{high} and B220$^+$Ig^{low} gates (*right*). These are representative plots for $n = 4$ tg(−) and $n = 3$ VH3H9 tg mice.

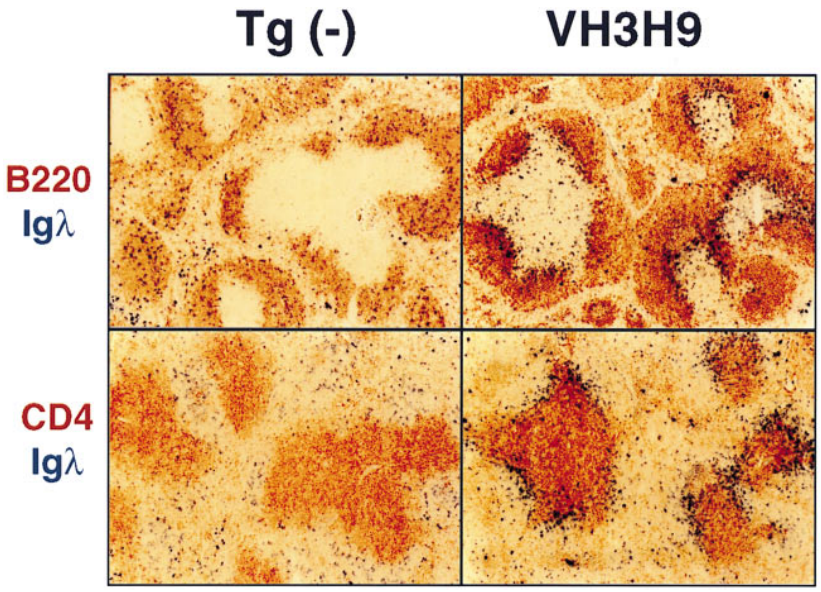

Figure 4. VH3H9/λ B cells accumulate at the T–B interface. Spleen sections from Tg(−) (*left*) and VH3H9 (*right*) mice were stained with anti-λ-AP and either anti-B220-biotin (*top*) or anti-CD4-biotin (*bottom*). A similar staining pattern was observed when anti-CD8-biotin was included with anti-CD4-biotin (data not shown). Avidin-HRP was used as a secondary step for the biotinylated reagents. HRP and AP were developed using the substrates, 3-amino-9-ethylcarbazole (*red*) and Fast-Blue BB base (*blue*), respectively. These are representative sections from $n = 15$ Tg(−) and $n = 19$ VH3H9 mice. Original magnification: 100.

in the bone marrow (2, 32). Thus, the bcl-2 tg protects B cells from deletion, but does not protect them from maturational arrest. The anti-dsDNA B cells are unique in that they are present in the periphery with an immature phenotype in the absence of a bcl-2 tg.

Anti-dsDNA B Cells Have a Reduced Lifespan. The in vivo lifespan of a B cell can be estimated by continuously labeling mice with the thymidine analogue BrdU, and then measuring the incorporation of BrdU-labeled cells into the splenic population (4, 52). A population that is rapidly turning over will be replaced more quickly with labeled cells from the bone marrow. Studies of BALB/c splenic B cell turnover rates have estimated that B cells have an average lifespan of 3–4 wk (4). To estimate the lifespan of anti-dsDNA B cells, tg(−) and VH3H9 tg mice were labeled with BrdU for 8 d and then the incorporation of BrdU was measured using flow cytometry. We chose to analyze the 8-d time point since this is when relatively few B cells will be labeled, and cells with an increased turnover rate will be readily apparent (4, 26). To assess the lifespan of the anti-dsDNA population of cells, we examined BrdU incorporation in the λ^+ subset. Fig. 3 *A* demonstrates that among the λ^+ cells, the frequency of BrdU-labeled cells is significantly higher in VH3H9 tg mice than in tg(−) mice (63.1 ± 5.6% versus 9.5 ± 0.4%), suggesting that the anti-dsDNA B cells have a decreased in vivo lifespan. Alternatively, the increased BrdU uptake in this population could be due to the active proliferation of the λ^+ B cells in vivo. To address this, we pulsed VH3H9 tg and tg(−) mice with BrdU for 2 h and then measured the uptake of BrdU in the splenic B cell populations. This is a time point when actively proliferating cells will take up BrdU, but is not a long enough period for replacement of cells from the bone marrow pool (52). We were unable to detect BrdU label in the λ^+ B cells in VH3H9 tg mice spleens. Labeling was analyzed and detected in the rapidly dividing populations of the bone marrow, thus ensuring that the mice did receive BrdU (data not shown). Together, these data suggest that the increased BrdU labeling of the VH3H9/λ B cells is due to their decreased in vivo lifespan.

Given that there are many κ L chains in addition to λ1 that can pair with the VH3H9 H chain to generate anti-dsDNA B cells, we predicted that they too may exhibit a decreased lifespan. Since we do not have L chain–specific reagents to detect these B cells (as we do for λ1), we used the phenotype of Ig^{low} to distinguish these cells. The λ^+ cells are included within the Ig^{low} cells, comprising 20–30% of this subset. Ig^{low} cells in tg(−) and VH3H9 tg mice were defined by gating on cells stained with either IgM and IgD (Fig. 3 *B*) or with only IgM (data not shown); both approaches yielded similar results. As shown in Fig. 3 *B*, the majority of the B cells in VH3H9 tg mice have approximately the same amount of BrdU incorporation as the tg(−) B cells. However, when we gate on the Ig^{low} subset of cells, 57.7 ± 5.1% of the tg B cells are labeled. These data are consistent with the idea that there are Ig^{low} κ^+ cells in VH3H9 tg mice that are dsDNA reactive, and these also have a rapid turnover rate. Interestingly, when we look in tg(−) mice, the Ig^{low} B cells are present, although at a much reduced frequency (<5% of the B cells). The Ig^{low} cells that we do detect have a slight increase in BrdU labeling (16%); however, this is much lower than that seen in the VH3H9 Ig^{low} B cells (62%). It is possible that the frequency of autoreactive B cells in tg(−) mice is too low to detect by these means, underscoring the advantage of using the VH3H9 tg to track these cells.

In the HEL B cell tolerance model, an increased in vivo turnover rate has been hypothesized to be a mechanism that maintains tolerance to self Ags (4). However, it is unclear whether this is dependent upon competition with nonautoreactive B cells or an intrinsic property of anergic B cells (4, 13). Here we have shown that when anti-dsDNA B cells are present in a polyclonal repertoire, they are short lived. Importantly, in another anti-dsDNA Ig tg model

(VH3H9 H chain with a mutated λ2 L chain), where the repertoire is monoclonal by virtue of the Rag-$2^{-/-}$ background, we have shown that anti-dsDNA B cells still exhibit a decreased lifespan (53). Therefore, we favor the interpretation that anti-dsDNA B cells are dying rapidly due to their exposure to antigen without receiving appropriate T cell help, rather than competition from nonautoreactive B cells.

Anti-dsDNA B Cells Are Located at the T–B Interface of the Splenic White Pulp. Lymphocytes are organized into discrete structures within the splenic architecture. Resting T and B cells segregate into the inner periarteriolar lymphoid sheath (inner PALS or T cell zone) and outer PALS (B cell follicle) within the spleen. To address where the short-lived anti-dsDNA B cells are located within the splenic architecture, spleen sections from tg(−) and VH3H9 tg mice were stained with anti-λ, anti-B220, and anti-CD4 to mark B and T zones, respectively (Fig. 4). In tg(−) mice, λ^+ B cells are scattered throughout the B cell area in the follicle as well as in the red pulp, but are not detected within the T zone. In contrast, the λ^+ anti-dsDNA B cells in the VH3H9 tg mouse are found clustered at the T–B interface in the B cell follicle, as well as in the T cell zone (Fig. 4).

These data are reminiscent of those obtained from the HEL system, where under some circumstances, anergic B cells have been reported to be excluded from the B cell follicle and accumulate in the inner PALS where they persist for only a few days (12, 13, 54). When using B220, both anti-HEL and anti-dsDNA B cells appear to accumulate at the T–B interface. However, staining with anti-CD4 to mark the T cell zone reveals that the anti-dsDNA B cells, contrary to anergic B cells in the HEL model, are present in the follicle, accumulating at the T zone proximal end (Fig. 4). Whether this distinction is important is presently not clear, nor is the relationship between follicular localization and lifespan (13, 54). Cyster et al. suggest that the follicle may provide growth factors or critical cell contacts that B cells require for survival and that these factors are not present or are too dilute at the edge of the T cell zone to be effective (55). Alternatively, Fulcher et al. propose that follicular localization and lifespan are determined by the degree of receptor engagement and availability of T cell help (54).

The localization of anti-dsDNA B cells is particularly intriguing within the framework of the model proposed by Rothstein et al. for B cell activation in the inner PALS (56). This model is based on immunohistochemical studies that identified IgG2a and rheumatoid factor B cells in the inner PALS of *lpr/lpr* mice, as well as data from the Goodnow lab which suggest that anergic B cells are Fas sensitive when given appropriate T help, regardless of Ig engagement (as opposed to conventional B cells that are Fas resistant in the presence of T help and Ig engagement) (57–59). The model further predicts that autoantibodies that arise in *lpr/lpr* mice may be a consequence of the inability to execute Fas-mediated apoptosis of anergic cells. Importantly for this model, we show that the anti-dsDNA B cells that are present in nonautoimmune animals are located at or near the PALS. Studies are underway to define the role that Fas-mediated apoptosis plays in the elimination of anti-dsDNA B cells once they have been reactivated and to determine if they form antibody-forming cells at this site in *lpr/lpr* mice.

Increased Frequency of λ^+ B Cells in VH3H9 tg Mice. λ^+ B cells are not only present in the periphery of VH3H9 tg mice, but they are present at a twofold higher frequency than in the tg(−) controls, despite the fact that VH3H9/λ1 B cells are autoreactive and have an increased turnover rate (Fig. 5). What could account for this seemingly surprising result? Pulsing mice with BrdU showed that the increased number of VH3H9/λ B cells is not simply due to their proliferation in the periphery (data not shown). Another possibility is that the VH3H9/λ B cells are positively selected (on some unidentified ligand) in the bone marrow. In support of this, there is a twofold increase in λ^+ B cells in the VH3H9 tg bone marrow over tg(−) bone marrow (Fig. 5). Alternatively, the increased λ frequency may be the consequence of receptor editing where λs represent the end result of multiple L chain rearrangement attempts (19, 33). The scenario we favor for an autoreactive Ig in VH3H9 tg mice is that after rearrangement at the κ loci is exhausted, λ rearrangement occurs, completing receptor editing. The $\lambda 1^+$ B cells that are generated are not deleted; rather, they persist in a compromised state.

Interestingly, when we compare the frequency of λ-expressing B cells in VH3H9 and tg(−) mice, the frequency is highest in the bone marrow and then decreases in the spleen. This is indicative of the loss of B cells from the bone marrow and recruitment into the long-lived splenic B cell pool (60). The frequency of λs changes only slightly between the spleen and lymph node in tg(−) mice; however, it decreases by half from the VH3H9 spleen to the lymph node

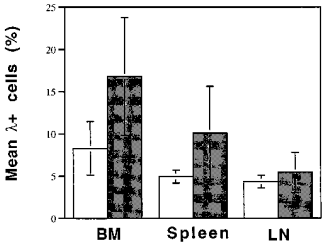

Figure 5. Increased frequency of λ^+ B cells in VH3H9 tg mice. Bone marrow (*BM*; *left*), spleen (*middle*), and lymph node (*right*) cells from Tg(−) (*open bars*) and VH3H9 (*shaded bars*) mice were stained with anti-B220-biotin/streptavidin-Red670 and anti-λ-FITC or -PE. The percentage of $B220^+\lambda^+$ cells of total B cells for spleen and lymph node and percentage of $B220^+\lambda^+$ cells out of total $B220^+Ig^+$ cells in the bone marrow was determined by flow cytometry. The graph shows the mean percentage of $B220^+\lambda^+$ B cells. There is an increased frequency of λ^+ B cells in the VH3H9 spleen (10.1 ± 5.5% versus 5.0 ± 0.8%; $P = 0.0011$). There is also a greater frequency of λ^+ B cells in the VH3H9 bone marrow (16.8 ± 7.0% versus 8.3 ± 3.1%; $P = 0.0010$), but not in the lymph node (5.4 ± 2.4% versus 4.4 ± 0.7%; $P = 0.1139$). Interestingly, when we compare the frequency of λ-expressing B cells within a mouse, the frequency is highest in the bone marrow and then decreases in the spleen (VH3H9: 16.8 ± 7.0% versus 10.1 ± 5.5%; $P = 0.0087$; tg(−): 8.3 ± 3.1% versus 5.0 ± 0.8%; $P = 0.0017$). The frequency of λs changes only slightly between the spleen and lymph node in tg(−) mice (5.0 ± 0.8% versus 4.4 ± 0.7%; $P = 0.0251$); however, it decreases drastically from the VH3H9 spleen to the lymph node (10.1 ± 5.5% versus 5.4 ± 2.4%; $P = 0.0034$). $n = 14$ tg(−) mice and $n = 13$ VH3H9 tg mice.

(Fig. 5). The loss of λ^+ B cells between the spleen and lymph node in VH3H9 tg mice may be a consequence of their reduced half life, resulting from autoreactivity.

In conclusion, we have used Ig H chain tg mice to boost the frequency of anti-dsDNA B cells and follow their fate in the context of a polyclonal repertoire. This is important because it more accurately reflects the conditions under which serum autoantibodies are expressed in autoimmune disease. To this end, we used the VH3H9 H chain tg, which pairs with the endogenous Vλ1 L chain, to generate an anti-dsDNA Ab, thus enabling us to follow anti-dsDNA B cells using λ-specific reagents. We report that these anti-dsDNA B cells are not deleted in the bone marrow, but instead are present in the periphery where they exhibit features of immaturity and activation, an increased in vivo turnover rate, and altered splenic localization. The lack of detectable anti-dsDNA serum titers (23) suggests that anti-dsDNA B cells are actively regulated, which we show is manifested by their unique phenotype. What accounts for the presence of anti-dsDNA Abs in autoimmunity is unknown. Studies are underway to determine if the addition of cognate T cell help will rescue anti-dsDNA B cells and lead to the expression of secreted autoantibodies.

We thank Dr. Andrew Caton and Eden Haverfield for critical reading of the manuscript, Dr. Andrew Caton for sequencing analysis, Dr. Garnett Kelsoe for help with setting up the histology staining protocol, Dr. Clayton Buck for use of his cryostat and microscope, Sudhir Nayak for help with the graphics, and Deepa Kurian for genotyping the mice. In addition, we acknowledge Drs. Randy Hardy and John Kearney for valuable reagents and discussion.

Services provided by the Wistar Institute staff were supported by the Core grant No. CA10815 and by grants from the National Institutes of Health (5R01 AI32137-06), the Arthritis Foundation, and the Pew Charitable Trust to J. Erikson. L. Mandik-Nayak is supported by the Wistar Training grant CA-09171. H. Noorchashm and A. Eaton are supported by the National Cancer Institute Training grant 2T32CA09140.

Address correspondence to Dr. Jan Erikson, The Wistar Institute, Rm 273, 3601 Spruce St., Philadelphia, PA 19104. Phone: 215-898-3823; FAX: 215-573-9053; E-mail: jan@wista.wistar.upenn.edu

Received for publication 17 June 1997 and in revised form 14 August 1997.

References

1. Nemazee, D.A., and K. Bürki. 1989. Clonal deletion of B lymphocytes in a transgenic mouse bearing anti-MHC class I antibody genes. *Nature (Lond.).* 337:562–566.
2. Hartley, S.B., J. Crosbie, R. Brink, A.B. Kantor, A. Basten, and C.C. Goodnow. 1991. Elimination from peripheral lymphoid tissues of self-reactive B lymphocytes recognizing membrane-bound antigens. *Nature (Lond.).* 353:765–769.
3. Goodnow, C.C., J. Crosbie, S. Adelstein, T.B. Lavoie, S.J. Smith-Gill, R.A. Brink, H. Pritchard-Briscoe, J.S. Wottersponn, R.H. Loblay, K. Raphael, et al. 1988. Altered immunoglobulin expression and functional silencing of self-reactive B lymphocytes in transgenic mice. *Nature (Lond.).* 334:676–682.
4. Fulcher, D.A., and A. Basten. 1994. Reduced life span of anergic self-reactive B cells in a double-transgenic model. *J. Exp. Med.* 179:125–134.
5. Hertz, M., and D. Nemazzee. 1997. BCR ligation induces receptor editing in IgM+IgD− bone marrow B cells in vitro. *Immunity.* 6:429–436.
6. Chen, C., E.L. Prak, and M. Weigert. 1997. Editing disease-associated autoantibodies. *Immunity.* 6:97–105.
7. Theofilopoulos, A.N., and F.J. Dixon. 1985. Murine models of systemic lupus erythematosus. *Adv. Immunol.* 37:269–390.
8. Shlomchik, M., M. Mascelli, H. Shan, M.Z. Radic, D. Pisetsky, A. Marshak-Rothstein, and M. Weigert. 1990. Anti-DNA antibodies from autoimmune mice arise by clonal expansion and somatic mutation. *J. Exp. Med.* 171:265–297.
9. Radic, M.Z., M.A. Mascelli, J. Erikson, H. Shan, and M. Weigert. 1991. Ig H and L chain contributions to autoimmune specificities. *J. Immunol.* 146:176–182.
10. Roark, J.H., C.L. Kuntz, K.-A. Nguyen, A.J. Caton, and J. Erikson. 1995. Breakdown of B cell tolerance in a mouse model of SLE. *J. Exp. Med.* 181:1157–1167.
11. Ibrahim, S.M., M. Weigert, C. Basu, J. Erikson, and M.Z. Radic. 1995. Light chain contribution to specificity in anti-DNA antibodies. *J. Immunol.* 155:3223–3233.
12. Cyster, J.G., S.B. Hartley, and C.C. Goodnow. 1994. Competition for follicular niches excludes self-reactive cells from the recirculating B-cell repertoire. *Nature (Lond.).* 371:389–395.
13. Cyster, J.G., and C.C. Goodnow. 1995. Antigen-induced exclusion from follicles and anergy are separate and complementary processes that influence peripheral B cell fate. *Immunity.* 3:691–701.
14. Chen, C., Z. Nagy, M.Z. Radic, R.R. Hardy, D. Huszar, S.A. Camper, and M. Weigert. 1995. The site and stage of anti-DNA B cell deletion. *Nature (Lond.).* 373:252–255.
15. Gay, D., T. Saunders, S. Camper, and M. Weigert. 1993. Receptor editing: an approach by autoreactive B cells to escape tolerance. *J. Exp. Med.* 177:999–1008.
16. Iliev, A., L. Spatz, S. Ray, and B. Diamond. 1994. Lack of allelic exclusion permits autoreactive B cells to escape deletion. *J. Immunol.* 153:3551–3556.
17. Tsao, B.P., A. Chow, H. Cheroutre, Y.W. Song, M.E. McGrath, and M. Kroneberg. 1993. B cells are anergic in transgenic mice that express IgM anti-DNA antibodies. *Eur. J. Immunol.* 23:2332–2339.
18. Hagman, J., D. Lo, L.T. Doglio, J.J. Hackett, C.M. Rudin,

D. Haasch, R. Brinster, and U. Storb. 1989. Inhibition of immunoglobulin gene rearrangement by the expression of a λ2 transgene. *J. Exp. Med.* 169:1911–1929.
19. Tiegs, S.L., D.M. Russell, and D. Nemazee. 1993. Receptor editing in self-reactive bone marrow B cells. *J. Exp. Med.* 177:1009–1020.
20. Spatz, L., V. Saenko, A. Iliev, L. Jones, L. Geskin, and B. Diamond. 1997. Light chain usage in anti–double stranded DNA B cell subsets: role in cell fate determination. *J. Exp. Med.* 185:1317–1326.
21. Tan, E.M., E.K.L. Chan, K.F. Sullivan, and R.L. Rubin. 1988. Antinuclear antibodies (ANAs): diagnostically specific immune markers and clues toward the understanding of systemic autoimmunity. *Clin. Immunol. Immunopathol.* 47:121–141.
22. Condemi, J.J. 1992. The autoimmune diseases. *JAMA (J. Am. Med. Assoc.).* 268:2882–2892.
23. Erikson, J., M.Z. Radic, S.A. Camper, R.R. Hardy, C. Carmack, and M. Weigert. 1991. Expression of anti-DNA immunoglobulin transgenes in non–autoimmune mice. *Nature (Lond.).* 349:331–334.
24. Radic, M.Z., J. Erikson, S. Litwin, and M. Weigert. 1993. B lymphocytes may escape tolerance by revising their antigen receptors. *J. Exp. Med.* 177:1165–1173.
25. Hardy, R.R., C.E. Carmack, S.A. Shinton, J.D. Kemp, and K. Hayakawa. 1991. Resolution and characterization of pro–B and pre–B cell stages in normal mouse bone marrow. *J. Exp. Med.* 173:1213–1225.
26. Allman, D.M., S.E. Ferguson, V.M. Lentz, and M.P. Cancro. 1993. Peripheral B cell maturation. II. Heat-stable antigen hi splenic B cells are an immature developmental intermediate in the production of long-lived marrow-derived B cells. *J. Immunol.* 151:4431–4444.
27. Jacob, J., R. Kassir, and G. Kelsoe. 1991. In situ studies of the primary immune response to (4-hydroxy-3-nitrophenyl)acetyl. I. The architecture and dynamics of responding cell populations. *J. Exp. Med.* 173:1165–1175.
28. Lane, P., T. Brocker, S. Hubele, E. Padovan, A. Lanzavecchia, and F. McConnell. 1993. Soluble CD40 ligand can replace the normal T cell–derived CD40 ligand signal to B cells in T cell–dependent activation. *J. Exp. Med.* 177:1209–1213.
29. Stark, S., and A.J. Caton. 1991. Antibodies that are specific for a single amino acid interchange in a protein epitope use structurally distinct variable regions. *J. Exp. Med.* 174:613–624.
30. Roark, J.H., C.L. Kuntz, K.-A. Nguyen, L. Mandik, M. Cattermole, and J. Erikson. 1995. B cell selection and allelic exclusion of an anti-DNA immunoglobulin transgene in MRL-*lpr*/*lpr* mice. *J. Immunol.* 154:4444–4455.
31. Cooke, M.P., A.W. Heath, K.M. Shokat, Y. Zeng, F.D. Finkelman, P.S. Linsley, M. Howard, and C.C. Goodnow. 1994. Immunoglobulin signal transduction guides the specificity of B cell–T cell interactions and is blocked in tolerant self-reactive B cells. *J. Exp. Med.* 179:425–438.
32. Hartley, S.B., M.P. Cooke, D.A. Fulcher, A.W. Harris, S. Cory, A. Basten, and C.C. Goodnow. 1993. Elimination of self-reactive B lymphocytes proceeds in two stages: Arrested development and cell death. *Cell.* 72:325–335.
33. Prak, E.L., M. Trounstine, D. Huszar, and M. Weigert. 1994. Light chain editing in κ-deficient animals: a potential mechanism of B cell tolerance. *J. Exp. Med.* 180:1805–1815.
34. Chen, C., M.Z. Radic, J. Erikson, S.A. Camper, S. Litwin, R.R. Hardy, and M. Weigert. 1994. Deletion and editing of B cells that express antibodies to DNA. *J. Immunol.* 152: 1970–1982.
35. Hang, L., A.N. Theofilopoulos, R.S. Balderas, S.J. Francis, and F.J. Dixon. 1984. The effect of thymectomy on lupus-prone mice. *J. Immunol.* 132:1809–1813.
36. Jabs, D.A., C.L. Burek, Q. Hu, R.C. Kuppers, B. Lee, and R.A. Pendergast. 1992. Anti-CD4 monoclonal antibody therapy suppresses autoimmune disease in MRL/Mp-*lpr*/*lpr* mice. *Cell. Immunol.* 141:496–507.
37. Wofsy, D., J.A. Ledbetter, P.L. Hendler, and W.E. Seaman. 1985. Treatment of murine lupus with monoclonal anti–T cell antibody. *J. Immunol.* 134:852–857.
38. Nitschke, L., R. Carsetti, B. Ocker, G. Kohler, and M. Lamers. 1997. CD22 is a negative regulator of B-cell receptor signalling. *Curr. Biol.* 7:133–143.
39. Molina, H., T. Kinoshita, K. Inque, J.-C. Carel, and V.M. Holers. 1990. A molecular and immunochemical characterization of mouse CR2: evidence for a single gene model of mouse complement receptors 1 and 2. *J. Immunol.* 145:2974–2983.
40. Dorken, B., G. Moldenhauer, A. Pezzutto, R. Schwartz, A. Feller, S. Kiesel, and L.M. Nadler. 1986. HD39 (B3), a B lineage–restricted antigen whose cell surface expression is limited to resting and activated human B lymphocytes. *J. Immunol.* 136:4470–4479.
41. Kikutani, H., M. Suemura, H. Owaki, H. Nakamura, R. Sato, K. Yamasaki, E. Barsumian, R. Hardy, and T. Kishimoto. 1986. Fcε receptor, a specific differentiation marker transiently expressed on mature B cells before isotype switching. *J. Exp. Med.* 164:1455–1469.
42. Ahearn, J.M., M.B. Fischer, D. Croix, S. Goerg, M. Ma, J. Xia, X. Zhou, R.G. Howard, T.L. Rothstein, and M.C. Carroll. 1996. Disruption of the Cr2 locus results in a reduction of B-1a cells and in an impaired B cell response to T-dependent antigen. *Immunity.* 4:251–262.
43. O'Keefe, T.L., G.T. Williams, S.L. Davies, and M.S. Neuberger. 1996. Hyperresponsive B cells in CD22-deficient mice. *Science (Wash. DC).* 274:798–801.
44. Sato, S., A.S. Miller, M. Inaoki, C.B. Bock, P.J. Jansen, M.L.K. Tang, and T.F. Tedder. 1996. CD22 is both a positive and negative regulator of B lymphocyte antigen receptor signal transduction: altered signaling in CD22-deficient mice. *Immunity.* 5:551–562.
45. Fearon, D.T., and R.H. Carter. 1995. The CD19/CR2/TAPA-1 complex of B lymphocytes: linking natural to acquired immunity. *Annu. Rev. Immunol.* 13:127–149.
46. Nadler, L.M., K.C. Anderson, G. Marti, M. Bates, E. Park, J.F. Daley, and S.F. Schlossman. 1983. B4, a human B lymphocyte–associated antigen expressed on normal, mitogen-activated, and malignant B lymphocytes. *J. Immunol.* 131:244–250.
47. Camp, R.L., T.A. Kraus, M.L. Birkeland, and E. Pure. 1991. High levels of CD44 expression distinguish virgin from antigen-primed B cells. *J. Exp. Med.* 173:763–766.
48. Hathcock, K.S., H. Hirano, S. Murakami, and R.J. Hodes. 1993. CD44 expression on activated B cells: differential capacity for CD44-dependent binding to hyaluronic acid. *J. Immunol.* 151:6712–6722.
49. Roehm, N.W., H.J. Leibson, A. Zlotnik, J. Kappler, P. Marrack, and J.C. Cambier. 1984. Interleukin-induced increase in Ia expression by normal mouse B cells. *J. Exp. Med.* 160: 679–694.
50. Mobley, J.L., and M.O. Dailey. 1992. Regulation of adhesion molecule expression by CD8 T cells in vivo. I. Differen-

tial regulation of gp90MEL-14, Pgp-1, LRA-1, and VLA-4α during the differentiation of cytotoxic T lymphocytes induced by allografts. *J. Immunol.* 148:2348–2356.
51. Gallatin, W.M., I.L. Weissman, and E.C. Butcher. 1983. A cell-surface molecule involved in organ-specific homing of lymphocytes. *Nature (Lond.).* 304:30–34.
52. Chan, E.Y.T., and I.C.M. MacLennan. 1993. Only a small proportion of splenic B cells in adults are short-lived virgin cells. *Eur. J. Immunol.* 23:357–363.
53. Roark, J.H., A. Bui, K.-A. Nguyen, L. Mandik, and J. Erikson. 1997. Persistence of functionally compromised anti-dsDNA B cells in the periphery of non-autoimmune mice. *Int. Immunol.* In press.
54. Fulcher, D.A., A.B. Lyons, S.L. Korn, M.C. Cooke, C. Koleda, C. Parish, B. Fazekas de St. Groth, and A. Basten. 1996. The fate of self-reactive B cells depends primarily on the degree of antigen receptor engagement and availability of T cell help. *J. Exp. Med.* 183:2313–2328.
55. Cyster, J. 1997. Signaling thresholds and interclonal competition in preimmune B-cell selection. *Immunol. Rev.* 156:87–101.
56. Jacobson, B.A., T.L. Rothstein, and A. Marshak-Rothstein. 1997. Unique site of IgG2a and rheumatoid factor production in MRL/lpr mice. *Immunol. Rev.* 156:103–110.
57. Jacobson, B.A., D.J. Panka, K.-A.T. Nguyen, J. Erikson, A.K. Abbas, and A. Marshak-Rothstein. 1995. Anatomy of autoantibody production: dominant localization of antibody-producing cells to T cell zones in Fas-deficient mice. *Immunity.* 3:509–519.
58. Rathmell, J.C., M.P. Cooke, W.Y. Ho, J. Grein, S.E. Townsend, M.M. Davis, and C.C. Goodnow. 1995. CD95 (Fas)-dependent elimination of self-reactive B cells upon interaction with CD4+ T cells. *Nature (Lond.).* 376:181–184.
59. Rothstein, T.L., J.K.M. Wang, D.J. Panka, L.C. Foote, Z. Wang, B. Stanger, H. Cui, S.-T. Ju, and A. Marshak-Rothstein. 1995. Protection against Fas-dependent Th1-mediated apoptosis by antigen receptor engagement in B cells. *Nature (Lond.).* 374:163–165.
60. Osmond, D.G. 1986. Population dynamics of bone marrow B lymphocytes. *Immunol. Rev.* 93:103–124.